

Application of the Time of Flight Technique for Lifetime Measurements with Relativistic Beams of Heavy Nuclei

A. Chester, P. Adrich, A. Becerril, D. Bazin, C. M. Campbell,
J. M. Cook, D.-C. Dinca,¹ W.F. Mueller, D. Miller, V. Moeller
R. P. Norris, M. Portillo, K. Starosta,* A. Stolz, J. R. Terry
H. Zwahlen, C. Vaman

*National Superconducting Cyclotron Laboratory and
Department of Physics and Astronomy, Michigan State University,
164 S. Shaw Lane, East Lansing, Michigan 48825-1321*

A. Dewald

*Institute for Nuclear Physics, University of Cologne, Zùlpicher Str. 77, D-50937
Köln, Germany*

Abstract

A novel method for picosecond lifetime measurements of excited γ -ray emitting nuclear states has been developed for fast beams from fragmentation reactions. A test measurement was carried out with a beam of ^{124}Xe at an energy of ~ 55 MeV/u. The beam ions were Coulomb excited to the 2_1^+ state on a movable target. Excited nuclei emerged from the target and decayed in flight after a distance related to the lifetime. A stationary degrader positioned downstream with respect to the target was used to further reduce the velocity of the excited nuclei. As a consequence, the γ -ray decays from the 2_1^+ excited state that occurred before or after traversing the degrader were measured at a different Doppler shift. The γ -ray spectra were analyzed from the forward ring of the Segmented Germanium Array; this ring positioned at 37° simultaneously provides the largest sensitivity to changes in β and the best energy resolution. The ratio of intensities in the peaks at different Doppler shifts gives information about the lifetime if the velocity β is measured. The results and range of the application of the method are discussed.

* corresponding author: phone (517) 324-8138, fax: (517) 353-5967, e-mail: starosta@nscl.msu.edu

¹ present address: American Science & Engineering, Inc. 829 Middlesex Turnpike

1 Motivation

Electromagnetic transition matrix elements are vitally important for nuclear structure studies. These matrix elements can be extracted if the information on the transition rate or lifetime is available for the state of interest. Picosecond-range lifetimes of excited nuclear states which decay by γ -ray emission can be reliably measured using Doppler shift methods; in particular, the Recoil Distance Method, also known as the plunger technique, see for example Refs. [1,2].

Exciting research opportunities to study nuclei far from stability have opened recently at the National Superconducting Cyclotron Laboratory following the construction of the Coupled Cyclotron Facility [3]. These nuclei are produced in fragmentation reactions at primary beams energies of ~ 140 MeV/u [4]. The fragments of interest are selected and identified on an event by event basis using the A1900 magnetic spectrograph [5]. The relativistic energies of secondary beams result in significant Doppler shifts for γ -rays following the secondary reactions. In fact, the Doppler broadening of γ -ray peaks resulting from momentum distribution of the secondary reaction products as well as from γ -ray detector opening angles is known to be the limiting factor in the application of high-resolution spectroscopy in relativistic beam facilities [6]. The current paper reports on a method of utilizing these large Doppler shifts for picosecond lifetime measurements using a relativistic plunger technique.

2 Experimental Method

In the reported experiment a beam of ^{124}Xe at an initial energy of 140 MeV/u was provided by the Coupled Cyclotron Facility at the National Superconducting Cyclotron Laboratory [3]. The primary beam was degraded in the fragmentation target of the A1900 separator [5] and delivered at an average energy of 54.9 MeV/u to the plunger apparatus installed at the target position of the S800 spectrometer [7]. The A1900 momentum acceptance cut was set to 0.5% and it was estimated that the plastic scintillator detectors used downstream from the A1900 contributed less than 0.02% to the beam momentum spread.

In the plunger apparatus the beam ions were Coulomb excited to the 2_1^+ state on a movable ^{93}Nb target with a thickness of 91.5 mg/cm². Excited projectiles emerged from the target with velocity $\beta_H=0.278(1)$ and γ -decayed in flight after a distance governed by the lifetime of the ^{124}Xe first excited

state. A stationary 79.5 mg/cm^2 ^{27}Al degrader positioned downstream with respect to the target was used to further reduce the velocity of these excited nuclei to $\beta_L=0.178(1)$. The γ -ray intensity measurements were carried out using the Segmented Germanium Array SeGA [8] centered on the degrader foil. Four target-degrader distances of $d=15.8 \text{ mm}$, 10.5 mm , 5.3 mm and a contact between target and degrader foils at $d=0 \text{ mm}$ were investigated. The separation between target and the degrader was fixed using thin cylindrical aluminum spacers and the precision of the spacer length measurement was better than 0.1 mm .

Depending on whether the γ -ray decay occurred in flight between target and degrader or if the decay occurred after slowing down in the degrader, the γ -rays exhibited different Doppler shifts. The resulting γ -ray spectra shown in Fig. 1 exhibit two peaks; the higher-energy peak corresponds to the γ -rays emitted before traversing the degrader while the lower-energy peak corresponds to γ -rays emitted after the degrader. From the relative intensity of the peak areas as a function of target-degrader distance, the lifetime of the state can be inferred as discussed in Sec. 3.

After passing through the degrader the nuclei were analyzed in the S800 spectrometer. Coincidence events corresponding to a γ -ray detection in the SeGA array and a beam particle detection in the E1 plastic scintillator detector at the S800 focal plane [9] were recorded for off-line analysis. In addition, the number of particles detected by the S800 E1 plastic scintillator was monitored and stored in intervals of five-second; these data were used for normalization of γ -ray intensities measured at different target-degrader separations. The readouts from the S800 focal plane Ionization Chamber were present in the data stream and were used in the off-line analysis for particle identification discussed in Sec. 5.1. The average rates for the experiment were ~ 23000 particles per second at the S800 focal plane and ~ 1700 particles per second in SeGA with the SeGA/S800 coincidence rate of ~ 60 per second. The average live time of the data acquisition system was $\sim 98\%$ and constant for runs at different target-degrader separation.

An important difference between the plunger technique applications at intermediate energies of $\sim 55 \text{ MeV/u}$ reported in this paper and the analogous technique near the Coulomb barrier energies of $\sim 5 \text{ MeV/u}$ is a significant contribution from the reactions on the degrader to the measured γ -ray intensity. In the current work the experimental information on that contribution has been identified from a separate run with the ^{27}Al plunger degrader foil in place but with the excitation target removed from the field of view of the SeGA detectors. To assure that the beam energy in this run is matched to that of the runs at smaller target-degrader separations the beam passed through the 91.5 mg/cm^2 ^{93}Nb foil mounted $\sim 60 \text{ cm}$ upstream of the plunger degrader. From these data it has been verified that the γ -rays following the reactions on

the degrader are emitted at the Doppler shift corresponding to the velocity β_L and thus are indistinguishable from the γ -ray decays from excitation on the plunger target which are emitted after traversing the degrader. The impact of the reactions on the degrader on the extracted lifetime is discussed further below.

3 Lifetime Measurement with the Time of Flight Technique

Coulomb excitation at the 55 MeV/u energy of interest for the current experiment is known to be predominantly a single step process [10]. For a case of a single level without any feeding, the number N_H and N_L of γ rays detected for states decaying between the target and the degrader and downstream from the degrader, respectively, are given by the relations:

$$N_H(d) = \frac{I_0}{D_H} \int_{-(d+d_0+d_m)}^{-d_m} \varepsilon_H(z) \exp\left(-\frac{z+d+d_0+d_m}{D_H}\right) dz \quad (1)$$

$$N_L(d) = \frac{I_0}{D_L} \exp\left(-\frac{d+d_0+d_d}{D_H}\right) \int_{d_d-d_m}^{d_{max}} \varepsilon_L(z) \exp\left(-\frac{z-d_d+d_m}{D_L}\right) dz \quad (2)$$

with D_H and D_L being related to the lifetime τ through:

$$D_H = \tau c \frac{\beta_H}{\sqrt{1-\beta_H^2}} \quad (3)$$

$$D_L = \tau c \frac{\beta_L}{\sqrt{1-\beta_L^2}} \quad (4)$$

Above, I_0 stands for the number of states excited in the target, while $\varepsilon_H(z)$ and $\varepsilon_L(z)$ are the efficiencies for detection of γ rays emitted at point z for the decays between the target and the degrader and downstream from the degrader, respectively. For the distance parameters, d is the measured target/degrader separation, the d_0 is the offset between the measured and the true target/degrader separation, the d_m is the length by which the plunger degrader foil is misaligned with respect to the center of the γ -ray array, and d_d is the degrader thickness. The upper integration limit d_{max} in Eq. 2 corresponds to the largest distance from the target at which γ -ray decays can still be detected in the SeGA array. In the current experiment this distance is significantly larger than D_H and D_L and $d_{max} = \infty$ can safely be assumed. The symbols for the plunger target/degrader foil alignment are further explained in Fig. 2.

In Eq. 2 it has been assumed that the decays in the degrader occur at the projectile velocity β_H . This approximation is valid for the current experiment since the thickness of the degrader $d_d \approx 0.3$ mm is significantly smaller than $D_L \sim D_H \approx 5.5$ mm. For thick degraders, the relevant correction has to be determined based on the energy loss of the beam nuclei in the degrader; however, it should be noted, that such a correction is not going to alter the dependence of N_L on d , which is of interest for the lifetime measurement.

In Sec. 4 the efficiencies $\varepsilon_H(z)$ and $\varepsilon_L(z)$ simulated with the Monte Carlo GEANT4 code [11] are discussed; these simulations demonstrate that these efficiencies can be well approximated with a second order polynomial in z

$$\varepsilon(z) = \varepsilon_0 + \varepsilon_1 z + \varepsilon_2 z^2 \quad (5)$$

In this case:

$$N_H(d) = I_0 \left[\tilde{\varepsilon}_H \left(1 - \exp\left(-\frac{d + d_0}{D_H}\right) \right) + \epsilon_H(d) \right] \quad (6)$$

$$N_L(d) = I_0 \tilde{\varepsilon}_L \exp\left(-\frac{d + d_0 + d_d}{D_H}\right) \quad (7)$$

with

$$\tilde{\varepsilon}_H = \varepsilon_H(D_H - d_m) + \varepsilon_2 D_H^2 \quad (8)$$

$$\epsilon_H(d) = \varepsilon_H(D_H - d_m - d - d_0) - \varepsilon_H(D_H - d_m) \quad (9)$$

$$\tilde{\varepsilon}_L = \varepsilon_L(D_L + d_d - d_m) + \varepsilon_2 D_L^2 \quad (10)$$

If a d -independent contribution from reactions on the degrader N_D is taken into account the final formula for N_L reads:

$$N_L(d) = I_0 \tilde{\varepsilon}_L \exp\left(-\frac{d + d_0 + d_d}{D_H}\right) + N_D \quad (11)$$

It should be pointed out that the $N_L(d)$ depends exponentially on the target/degrader separation d , while there are d -dependent efficiency corrections to the number of decays between the target and the degrader N_H as given by Eqs. 6 and 9.

The above formulae demonstrate that the number of decays upstream and downstream from the degrader is defined by the target/degrader separation d and the velocity β_H between the target and the degrader. Thus, the lifetime of the state of interest can be extracted from the measured intensity variation

of N_H and N_L as a function of d if the velocity β_H is measured at the same time. The intensity variations of N_H and N_L as a function of d can be measured from the number of counts in the low- and high-energy component of the peak corresponding to the transition of interest normalized to the beam current integrated over the time of the run. The measurement of these experimental observables provides the basis for the current method of lifetime determination.

4 Efficiency of γ -ray detection

It is argued in the previous section that the dependence of the efficiency for γ -ray detection on the position of a decay along the beam axis is of importance for the application of the current method. Since relativistic effects have a significant impact on the γ -ray detection efficiency, this dependence has been studied for the purpose of the current experiment using a Monte Carlo GEANT4 [11] simulation code. The code was set up to include major parts of the plunger apparatus used in the experiment and provided segment energy deposits for detected γ -rays in a single simulated SeGA detector.

The following effects were taken into account in the simulations:

- The dependence of the solid angle covered by the detector on the position of the decay.
- Attenuation of the γ -ray flux by the elements of the plunger and the beam tube.
- The Doppler shift of the γ -ray energy depending on the source velocity and the direction of the γ -ray emission.
- The response of the detector to γ rays at Doppler shifted energies (monochromatic sources of radiation were assumed in the moving reference frame).
- The angular distribution of γ -rays in the source reference frame.
- The relativistic beaming of γ -ray in the laboratory reference frame from the source being in motion (so called “Lorentz boost”). The beaming can be seen from a relation between the γ -ray emission angle in the laboratory frame θ and the γ -ray emission angle θ' in the frame of a nucleus:

$$\cos \theta = \frac{\cos \theta' + \beta}{1 + \beta \cos \theta'}, \quad (12)$$

which result in the following relation

$$d\Omega = \frac{1 - \beta^2}{(1 + \beta \cos \theta')^2} d\Omega' = \frac{(1 - \beta \cos \theta)^2}{1 - \beta^2} d\Omega', \quad (13)$$

between the differential solid angles $d\Omega$ and $d\Omega'$ in the laboratory and the

moving frame of a nucleus, respectively. The ‘‘Lorentz boost’’ results in increased probability of a γ -ray emission in the direction of motion of the source despite of the forward/backward symmetry of the angular distribution in the moving reference frame.

It should be pointed out here that for the above items only the response of the detector to γ -rays at non-Doppler shifted energies, the change of the solid angle and the attenuation of the γ -ray flux by the experimental setup can be measured with calibration sources. All other effects can not be measured directly and need to be calculated.

The γ -ray efficiency has been evaluated for the current experiment assuming three different cases of angular distributions in the moving reference frame.

- The angular distribution with coefficients $a_2=-0.64$ and $a_4=-0.22$ resulting from the intermediate energy Coulomb excitation calculated for the current experimental conditions according to Ref. [12].
- The above angular distribution but attenuated due to the presence of odd-electron charged states to $a_2=-0.58$, $a_4=-0.13$ with the attenuation factor $G_2 = 4/5$ and $G_4 = 1/5$ calculated according to Refs. [13] and [14].
- Isotropic angular distribution.

The results of calculations for the target/degrader separation $d = 15.8$ mm are presented in Fig. 3. The discontinuity observed in this figure at $d = 0$ mm arises predominantly from the change of relativistic beaming after slowing down in the degrader. The efficiency increase as a function of z is understood from the fact that the points of decay in the considered range of z are closer to the detector in the SeGA ring at 37° as z increases. This is true at $\beta \sim 0.3$ for states with lifetimes on the order of tens of picoseconds which decay within a few centimeters away from the target. This assumption, however, has to be verified if longer lifetimes are investigated with the current method. The trends observed in Fig. 3 justify the second order approximation for the efficiency dependence on z employed in Sec. 3. The efficiency coefficients fitted to the simulation data are summarized in Tab. 1 and the resulting fits are plotted in Fig. 3.

5 Experimental Results

5.1 Particle Identification

Events that corresponded to the de-excitation process of ^{124}Xe were selected using a combination of SeGA [8] and detectors at the focal plane of the S800

spectrometer [7,9]. SeGA-S800 time coincidence was measured on an event-by-event basis starting when the SeGA array detected a γ -ray and stopping when the nucleus reached the E1 plastic scintillator at the focal plane of the S800 downstream from the degrader. The γ -ray energy dependent time gates compensating for a time-walk resulting from different signal amplitudes in the SeGA detectors were used off-line to improve the peak to background ratio. An S800 focal plane gate was created to select events that corresponded to a ^{124}Xe nucleus based on the measured energy loss recorded by the E1 plastic scintillator and the ion chamber. The final particle identification (PID) gate was a combination of the time-energy gate and the S800 focal plane gate. The improvement in the signal to noise ratio from the initial value of ~ 0.31 in the region corresponding to the two peaks to the final value of ~ 0.50 after the application of the particle identification gate can be seen in Fig. 4.

5.2 Velocity Measurement

The precision and accuracy of the β_H velocity measurement for the decays between the target and the degrader has a direct impact on the precision and accuracy of the lifetime measurement with the current technique, see Sec. 3. Below it is argued that from the Doppler shift of γ -ray energies emitted in flight, the error on the velocity measurement β_H given by a standard deviation σ can be reduced to less than 0.3%, and a precise lifetime can be extracted.

The SeGA detectors are electronically divided into 32 segments which form 8 slices at different polar angles θ [8]. Gamma-ray energies recorded in each of the 8 slices of individual SeGA detectors were used to measure velocity of the ^{124}Xe nuclei through the observed Doppler shift of the $E_0 = 354$ keV transition depopulating the 2^+ first excited state. The non-Doppler corrected spectra corresponding to the SeGA slices and the PID gate described in Sec. 5.1 were sorted for each target-degrader separation distance. The effect of the Doppler shift on the lower-energy peak corresponding to γ rays emitted after the degrader can be seen in Fig. 5 for a target-degrader separation $d=10.5$ mm.

Spectra corresponding to the de-excitation events recorded by each slice in the SeGA detectors were summed over the azimuthal angle φ and the centroids of the gamma-ray peaks of interest were measured at the corresponding value of the polar angle θ . The centroid data from these spectra were used to determine velocities β_H and β_L for the peaks representing γ -rays emitted before and after the degrader, respectively, for each target-degrader separation. These data were fit using the relativistic Doppler equation:

$$E = E_0 \frac{\sqrt{1 - \beta^2}}{1 - \beta \cos \theta} \quad (14)$$

by a least squares fitting method. The average decay position along the beam axis for the decays upstream and downstream from the degrader, z_H and z_L , respectively, were free parameters of these fits. The decay position z is related to the polar angle θ in Eq. 14 by the target-detector separation distance $L = 24$ cm and the detector segment angle in the array θ_0 :

$$\cos \theta = \frac{\cos \theta_0 - \frac{z}{L}}{\sqrt{1 - 2\left(\frac{z}{L}\right) \cos \theta_0 + \left(\frac{z}{L}\right)^2}}. \quad (15)$$

The result of the least squares fit for β_H and z_H is shown in Fig. 6 for a target-degrader separation of $d=10.5$ mm. The χ^2 contour plot shown in Fig. 7 provides evidence that velocity β_H can be measured with $\sim 0.3\%$ precision. The results of the β_H/z_H and β_L/z_L measurements are summarized in Tab. 2. The value of β_H adopted based on the measurements at three target/degrader separations of $d=5.3, 10.5$ and 15.8 mm is $\beta_H=0.278(1)$.

5.3 Normalized Intensity Measurement

For the intensity measurements as a function of target-degrader separation, the Doppler corrected spectra at a constant polar angle θ were summed over different azimuthal angles φ . Doppler corrections were performed separately for the high- and low-energy peaks with the corresponding measured values of β_H and z_H or β_L and z_L respectively. Fig. 8 demonstrates the improved energy resolution from the Doppler corrections for the spectrum corresponding to that shown in Fig. 5.

The number of counts in the high- and low-energy peaks were measured and recorded for each distance d . These SeGA photo-peak counts were normalized to the total number of nuclei detected by the S800 E1 scintillator from the recorded scalers. Since the deadtime of the data acquisition system was small ($\sim 2\%$) and equal for different target/degrader separations, no further corrections or normalizations were applied. The resulting normalized intensities are listed in Tab. 3.

5.4 Lifetime measurement for the 2_1^+ state in ^{124}Xe

It is indicated by Eq. 11 that the lifetime of the 2_1^+ state in ^{124}Xe can be extracted from the decay-curve data in the last column of Tab. 3 using an exponent plus a constant fit

$$N_L/N_0 = v \cdot \exp\left(-\frac{d}{D_H}\right) + u, \quad (16)$$

with

$$v = \frac{I_0}{N_0} \tilde{\varepsilon}_L \exp\left(-\frac{d_0 + d_d}{D_H}\right), \quad u = \frac{N_D}{N_0}. \quad (17)$$

In the above formulae all the efficiency and background factors are absorbed into the fitted constants. The results of the fit shown in Fig. 9 yield $D_H = 5.6_{-0.6}^{+0.8}$ mm which corresponds to $\tau = 64_{-8}^{+10}$ ps for $\beta_H = 0.278(1)$ in excellent agreement with a recent measurement of $\tau = 67.5(1.7)$ ps reported in Ref. [15].

The above procedure of extracting lifetime does not take into account the full experimental information provided by the measurement. A simultaneous fit to both components of the γ -ray transition of interest can be performed; it requires, however, a proper handling of the efficiency corrections which depend on the target/degrader separation for the decays upstream from the degrader.

For this simultaneous fit the formulae discussed in Sec. 3 can be written as

$$\begin{aligned} \frac{N_H}{N_0} &= p \left[1 - \exp\left(-\frac{d + d_0}{D_H}\right) \right] + \\ &\quad -q(d + d_0) + r(d + d_0)(d + d_0 + 2d_m - 2D_H) \\ \frac{N_L}{N_0} &= w \exp\left(-\frac{d + d_0}{D_H}\right) + u. \end{aligned} \quad (18)$$

with

$$p = \frac{I_0}{N_0} \tilde{\varepsilon}_H, \quad q = \frac{I_0}{N_0} \varepsilon_{1H}, \quad r = \frac{I_0}{N_0} \varepsilon_{2H}, \quad \text{and} \quad w = \frac{I_0}{N_0} \tilde{\varepsilon}_L \exp\left(-\frac{d_d}{D_H}\right). \quad (19)$$

The total $\chi^2 = \chi_H^2 + \chi_L^2$ is then minimized as a function of D_H , d_0 , d_m , p , q , r , u , and w constants.

In the current analysis the eight-parameter fit implied by Eqs. 18 to nine data points given in Tab. 3 is carried on as an exercise rather than a proper measurement. In practical applications additional data points at well chosen target/degrader separation are needed to constrain the fitted parameters. Here it was assumed that $d_m = 0$ and that the slope of the N_H/N_0 function is zero at $d \sim 15$ mm as suggested by the data points in Tab. 3.

The results of the simultaneous fit are sensitive to the d_0 parameter through the N_H/N_0 component. A fit with the d_0 parameter varied freely yields the $D_H = 5.6(6)$ mm and $d_0 = 2.4(4)$ mm. This value of d_0 seemed too large for the

current experimental conditions. A fit with the d_0 parameter constrained to less than 2.0 mm yields $D_H=5.5(7)$ mm, a value consistent with that obtained from the fit to the N_L/N_0 data alone. The results of the simultaneous fit with $d_0=2.0$ mm are shown in Fig. 10 together with the N_H/N_0 curve expected in the absence of the d -dependent efficiency corrections for the decays between the target and the degrader. The $w/p \sim 0.86$ ratio from this fit is consistent with the results of the Monte Carlo simulations discussed in Sec. 4 and presented in Fig. 3 and Tab. 1.

Figure 10 indicates that in a plunger experiment with the stationary degrader the efficiency change as a function of the target/degrader separation has a significant impact on the detected number of counts for the decays upstream from the degrader. The efficiency corrections for the decays upstream from the degrader can be measured if a sufficient number of data points at $d > D_H$ is provided. On the other hand the N_L/N_0 data are essentially free from the efficiency corrections for a large range of lifetimes. These factors are of significant importance and need to be taken into account in planning and executing relativistic plunger experiments.

6 Range of application for the method

The factor which is limiting the application of the method for short lifetimes is related predominantly to the thickness of the plunger excitation target and the degrader foil. Certainly, the lifetime of a state being studied has to be long enough for the excited nuclei to emerge from the target and decay in vacuum. A typical target thickness for experiments with relativistic beams is $\sim 100 \mu\text{m}$ which corresponds to ~ 1 ps at $\beta \sim 0.3$.

If thin excitation targets can be used in an experiment the $d_0 < D_H$ condition sets the limit for observing variations in N_H as a function of d according to Eq. 6. The minimization of d_0 is a well known challenge in plunger experiments; it requires that the target and the degrader foils are flat and parallel. This is achieved by careful stretching and alignment of the target and degrader foils. Currently the values of $d_0 < 10 \mu\text{m}$, corresponding to 0.3 ps at $\beta = 0.3$, are routinely achieved. However, it must be stressed that the targets of $\sim 10 \mu\text{m}$ thickness are essential for sub-picosecond lifetime measurements and that application of these targets necessarily results in reduced reaction yields.

The shortest lifetime which can be measured from the variation of N_L is defined by the degrader thickness entering the $d_0 + d_d < D_H$ condition from Eq. 7. The degrader thickness is selected to provide a change of the Doppler shift which is sufficient to resolve the components of the transition of interest emitted before and after traversing the degrader. For typical γ -ray detection

resolution in relativistic beam experiments of $\sim 2\%$ FWHM the degrader thickness of $\sim 300 \mu\text{m}$ is required. This sets the lifetime limit of more than 3 ps at $\beta \sim 0.3$. However, for such short lifetimes the decays at changing velocity within the degrader contribute significantly and peak shape modeling based on the stopping power of the degrader seems to be needed to account properly for the intensity balances. The contribution of the decays in the degrader decreases for longer lifetimes and seem to be negligible in the current analysis as demonstrated from experimental spectra shown in Fig. 8.

For the short lifetime measurements discussed above the efficiency changes as a function of the target/degrader separation are essentially negligible. However, these efficiency changes limit the application of the method for states with long lifetimes. It is estimated that the forward ring of the SeGA array at 37° can be used to detect decays up to 20 cm downstream from the degrader foil. For a significant fraction of the decays of interest to occur with this length the D_H has to be shorter by a factor of ~ 4 . This corresponds to the lifetime of $\tau \sim 500$ ps.

Based on the above discussion, the current technique can be applied to γ -ray emitting states with lifetimes between 5 and 500 ps. The above estimates do not take into account the relativistic time dilation which is a $\sim 10\%$ correction at $\beta \sim 0.3$ which allows to investigate shorter lifetimes. It seems possible to extend the method to sub-picosecond lifetime measurement, however, further careful studies are needed for such applications.

7 Choice of the relativistic plunger target/degrader materials

An important issue for the application of the current technique is a choice of the target and degrader materials. The thickness of the degrader is directly related to the constant contribution N_D to the intensity N_L used to determine the lifetime from Eq. 11 and 16. This arises from the fact that relativistic beams have enough energy to react on both, the plunger excitation target and the degrader. This is one of the essential differences between the current method and plunger applications near the Coulomb barrier for which reactions on the degrader can be, for many cases, completely eliminated by a proper choice of the degrader material. The precision of the N_D determination has a direct impact on the precision of the lifetime measurement. The precision of the lifetime measurement can be improved by minimizing the N_D , however, it is not essential for the application of the method to eliminate N_D completely.

The current approach for selecting the target and degrader material for relativistic plunger experiments is based on two principles:

- The cross section for the excitation process of interest has to be maximized on the target and minimized on the degrader. For example, if Coulomb excitations are used, the target and the degrader should be made out of high-Z and low-Z material, respectively. On the other hand, if fragmentation is used to populate the states of interest then the target and the degrader should be made out of low-Z and high-Z material, respectively.
- The thickness of the degrader has to be minimized preserving the change of velocity sufficient to resolve the Doppler-shifted components of the transition of interest emitted before and after traversing the degrader. Thus, the change of the Doppler shift from traversing the degrader has to be balanced against the γ -ray energy resolution for the peaks of interest. Since the energy resolution is determined by various factors [6] including solid angle for γ -ray detection and beam momentum spread, case by case studies are needed for planning a relativistic plunger experiment.

8 Conclusions

The experiment reported in the current paper provides a proof of principle for application of the time of flight technique for lifetime measurements with relativistic beams of heavy nuclei. The $\tau=64_{-8}^{+10}$ ps lifetime for the first excited 2_1^+ state in ^{124}Xe measured with the above relativistic plunger method is in an excellent agreement with the most accurately known value of $\tau=67.5(1.7)$ ps from recent Ref. [15]. Further development of the method for experiments with rare isotopes produced in projectile fragmentation reaction at the NSCL are planned. In particular a plunger device optimized for the fast beams at the NSCL is being constructed by the collaboration between the NSCL and the University of Cologne.

The advantage of the plunger method is in its relatively simple dependence on reaction kinematics and in the fact that it does not depend on reaction dynamics. Thus, in a plunger experiment, any excitation mechanism can be used for populating the state of interest while the lifetime information is extracted from a decay curve measured directly. Moreover, the lifetime information results from a series of measurements for which only relative properties of the experimental set-up need to be known or calibrated. In particular, the knowledge of the absolute set-up efficiency is not critical for accurate lifetime measurement.

The plunger method is not limited by isomer contamination of the beam. This makes it an ideal tool to explore odd-even and odd-odd nuclei, investigating in particular single-particle electromagnetic moments near closed shells in neutron rich nuclei for which the available information is scarce at present. It is estimated that plunger experiments require beam intensities of only 10^6

particle per second, so that knockout reactions with rare isotopes are possible.

Current applications of the plunger technique near the Coulomb barrier provide the most accurate electromagnetic transition rate measurements for picosecond lifetimes. Successful application of the relativistic plunger technique in fragmentation facilities provides an opportunity to explore new and untouched areas of rare isotopes far from stability.

9 Acknowledgments

This work has been partially supported by the (US) National Science Foundation Grant No. PHY01-10253 and by the BMBF (GERMANY) under contract No. 06K167.

References

- [1] D. B. Fossan and W. K. Warburton, in *Nuclear Spectroscopy and Reactions, Part C*, ed. J. Cerny, Academic Press, New York and London, (1974) p. 307.
- [2] R. Krücken, J. Res. Natl. Inst. Stand. Technol. 105 (2000) 53.
- [3] F. Marti, D. Poe, M. Steiner, J. Stetson, X.Y. Wu, *Proceedings of the 2001 Particle Accelerator Conference, Chicago, IL*, IEEE 01CH37268,(2001) 2557.
- [4] A. Stolz, T. Baumann, T. N. Ginter, D. J. Morrissey, M. Portillo, B. M. Sherrill, M. Steiner, and J. W. Stetson, Nucl. Instr. and Meth. Phys. Res. B 241 (2005) 858.
- [5] D. J. Morrissey, B. M. Sherrill, M. Steiner, A. Stolz and I. Wiedenhoever, Nucl. Instr. and Meth. Phys. Res. B 204 (2003) 90.
- [6] T. Glasmacher, Ann. Rev. Nucl. Part. Sci. 48, 1, (1998).
- [7] D. Bazin, J.A. Caggiano, B.M. Sherrill, J. Yurkon and A. Zeller, Nucl. Instr. and Meth. Phys. Res. B 204 (2003) 629.
- [8] W.F. Mueller, J.A. Church, T. Glasmacher, D. Gutknecht, G. Hackman, P.G. Hansen, Z. Hu, K.L. Miller and P. Quinn, Nucl. Instr. and Meth. Phys. Res. A 466 (2001) 492
- [9] J. Yurkon, D. Bazin, W. Benenson, D.J. Morrissey, B.M. Sherrill, D. Swan, R. Swanson and Nucl. Instr. and Meth. Phys. Res. A 422 (1999) 291.
- [10] A. Winther and K. Alder, Nucl. Phys. A 319 (1979) 518.

- [11] S. Agostinelli, J. Allison, K. Amako, J. Apostolakis, H. Araujo, P. Arcel, M. Asai, D. Axen, t, S. Banerjee, G. Barrand, F. Behner, L. Bellagamba, J. Boudreau, L. Broglia, A. Brunengo, H. Burkhardt, S. Chauvie, J. Chuma, R. Chytracek, G. Cooperman, G. Cosmo, P. Degtyarenko, A. Dell'Acqua, G. Depaola, D. Dietrich, R. Enami, A. Feliciello, C. Ferguson, H. Fesefeldt, G. Folger, F. Foppiano, A. Forti, S. Garelli, S. Giani, R. Giannitrapani, D. Gibin, J. J. Gmez Cadenas, I. Gonzalez, G. Gracia Abril, G. Greeniaus, W. Greiner, V. Grichine, A. Grossheim, S. Guatelli, P. Gumplinger, R. Hamatsu, K. Hashimoto, H. Hasui, A. Heikkinen, A. Howard, V. Ivanchenko, A. Johnson, F. W. Jones, J. Kallenbach, N. Kanaya, M. Kawabata, Y. Kawabata, M. Kawaguti, S. Kelner, P. Kent, A. Kimura, T. Kodama, R. Kokoulin, M. Kossov, H. Kurashige, E. Lamanna, T. Lampn, V. Lara, V. Lefebure, F. Lei, M. Liendl, W. Lockman, F. Longo, S. Magni, M. Maire, E. Medernach, K. Minamimoto, P. Mora de Freitas, Y. Morita, K. Murakami, M. Nagamatu, R. Nartallo, P. Nieminen, T. Nishimura, K. Ohtsubo, M. Okamura, S. O'Neale, Y. Oohata, K. Paech, J. Perl, A. Pfeiffer, M. G. Pia, F. Ranjard, A. Rybin, S. Sadilov, E. Di Salvo, G. Santin, T. Sasaki, N. Savvas, Y. Sawada, S. Scherer, S. Sei, V. Sirotenko, D. Smith, N. Starkov, H. Stoecker, J. Sulkimo, M. Takahata, S. Tanaka, E. Tcherniaev, E. Safai Tehrani, M. Tropeano, P. Truscott, H. Uno, L. Urban, P. Urban, M. Verderi, A. Walkden, W. Wander, H. Weber, J. P. Wellisch, T. Wenaus, D. C. Williams, D. Wright, T. Yamada, H. Yoshida and D. Zschesche, Nucl. Instr. Meth. A506, 250 (2003).
- [12] H. Olliver, T. Glasmacher, and A. E. Stuchbery, Phys. Rev. C68 (2003) 044312.
- [13] A.E. Stuchbery, A.N. Wilson, P.M. Davidson, A.D. Davies, T.J. Mertzimekis, S.N. Liddick, B.E. Tomlin and P.F. Mantica, Phys. Lett. B611 (2005) 81.
- [14] G. Goldring, in *Heavy Ion Collisions, vol. 3, ed. R. Bock, Noth-Holland, Amsterdam, New York, Oxford, (1982) p. 483.*
- [15] B. Saha, A. Dewald, O. Möller, R. Peusquens, K. Jessen, A. Fitzler, T. Klug, D. Tonev, P. von Brentano, J. Jolie, B. J. P. Gall, and P. Petkov, Phys. Rev. C 70 (2004) 034313.

Table 1

Coefficients for γ -ray efficiency $\varepsilon(z)$ dependence on the position of the point of decay z along the beam axis fitted according to Eq. 5 to the simulation data shown in Fig 3. See Sec. 4 for details.

angular distribution	$\varepsilon_0 H$	$\varepsilon_1 H$	$\varepsilon_2 H$	$\varepsilon_0 L$	$\varepsilon_1 L$	$\varepsilon_2 L$
Coulex	0.4852(5)	0.00451(6)	-0.000011(5)	0.4072(5)	0.00376(4)	0.000038(3)
attenuated Coulex	0.4718(5)	0.00404(6)	0.000002(5)	0.4140(5)	0.00310(4)	0.000048(3)
isotropic	0.5007(6)	0.00313(6)	0.000000(5)	0.4559(5)	0.00289(4)	0.000019(3)

Table 2

Result of β_H/z_H and β_L/z_L measurements as a function of the target/degrader separation d .

d	β_H	z_H [mm]	β_L	z_L [mm]
0.0			0.1784(2)	7.6(3)
5.3	0.2771(5)	1.3(5)	0.1784(3)	7.9(4)
10.5	0.2778(3)	-1.1(3)	0.1792(3)	8.3(4)
15.8	0.2774(5)	-6.7(5)	0.1792(4)	8.3(5)
∞			0.1779(4)	7.2(7)

Table 3

Normalized intensities for the high- and low-energy component of the $E_0 = 354$ keV $2_1^+ \rightarrow 0_1^+$ transition in ^{124}Xe measured in the current experiment as a function of the target/degrader separation d .

d	N_H/N_0	N_L/N_0
0.0	20(2)	80(1)
5.3	34(2)	53(2)
10.5	42(2)	44(1)
15.8	42(2)	38(1)
∞		38(2)

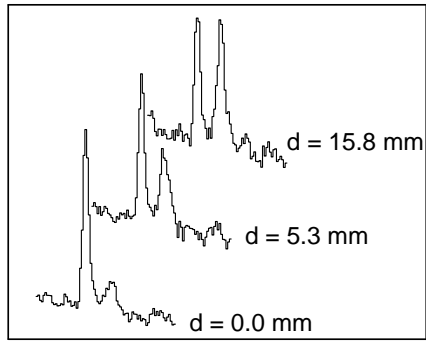


Fig. 1. Change of intensity as a function of the target-degrader distance for the two components of a Doppler-shifted γ -ray peak corresponding to the 354 keV transition from the first excited 2_1^+ state in ^{124}Xe . The higher- and lower-energy component of the peak corresponds to the decays upstream and downstream with respect to the plunger degrader foil, respectively. The variation of intensities of these two components as a function of the target/degrader separation is defined by the lifetime of the transition and the velocity β_H of the nuclei between the target and the degrader. The method reported in the current paper utilizes this variation for lifetime measurement of the 2_1^+ state in ^{124}Xe .

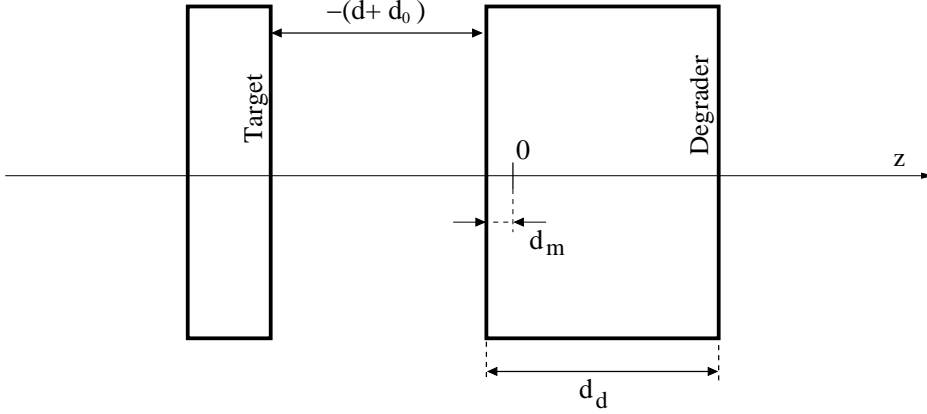


Fig. 2. Schematic alignment of the plunger excitation target and the degrader foil with respect to the center of the SeGA array. The distance d is the measured target/degrader separation, d_0 is the offset between the measured and the true target/degrader separation, d_m is the length by which the plunger degrader foil is misaligned with respect to the center of the γ -ray array, and d_d is the degrader thickness.

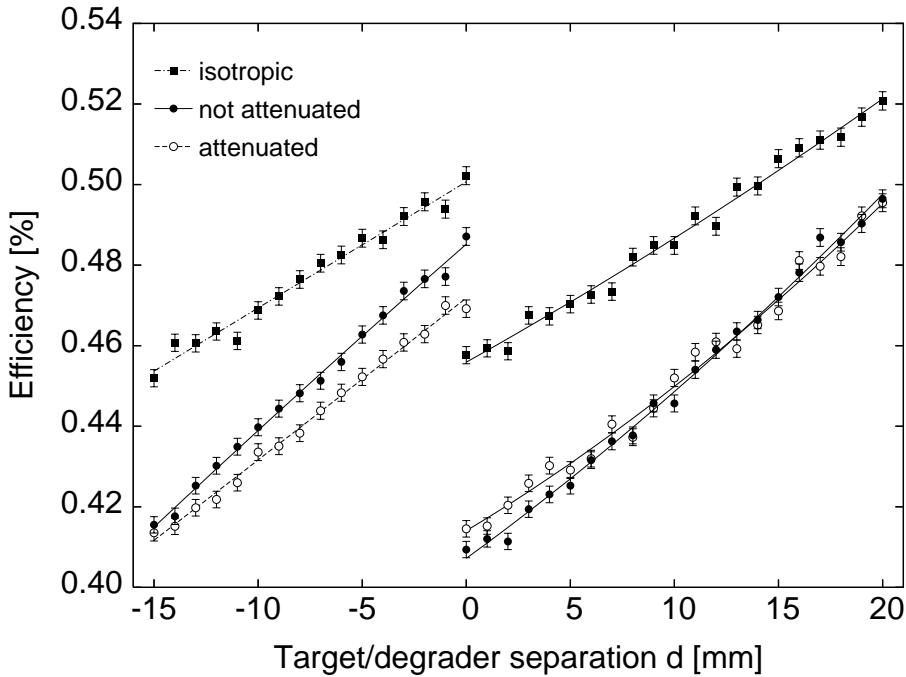


Fig. 3. Changes in γ -ray efficiency of a single SeGA detector at 37° as a function of the position of the decay along the beam axis for the target/degrader separation of $d = 15.8$ mm. Filled boxes/dashed-dotted line, filled circles/continuous line and open circles/dashed line are for the isotropic, not-attenuated and attenuated angular distribution in the moving reference frame of the decaying nuclei, respectively. The discontinuity at $d = 0$ mm arises predominantly due to the change of relativistic beaming after slowing down in the degrader. For details of the efficiency calculation see Sec. 4 and Tab. 1.

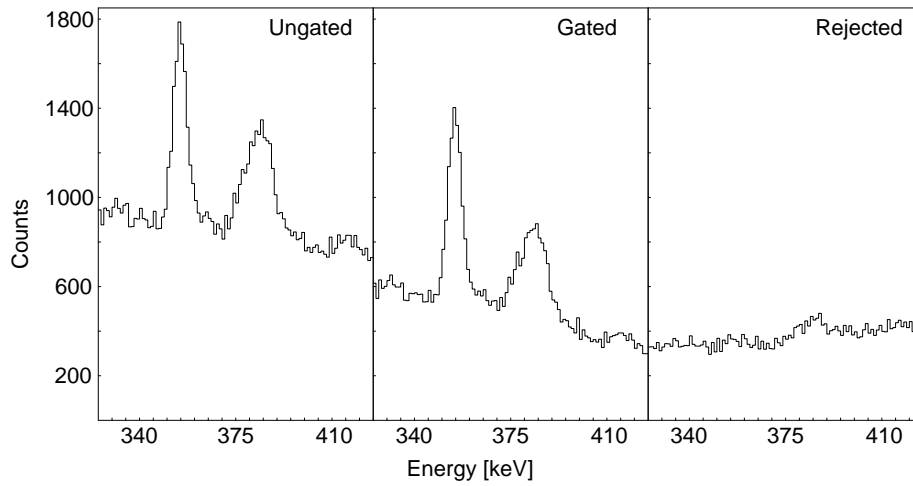


Fig. 4. Application of the PID gate to a Doppler corrected spectra at $d=10.5$ mm. The left panel shows the spectrum without the PID gate. The middle panel shows the same spectrum with the PID gate applied. The right panel shows events rejected by the PID gate.

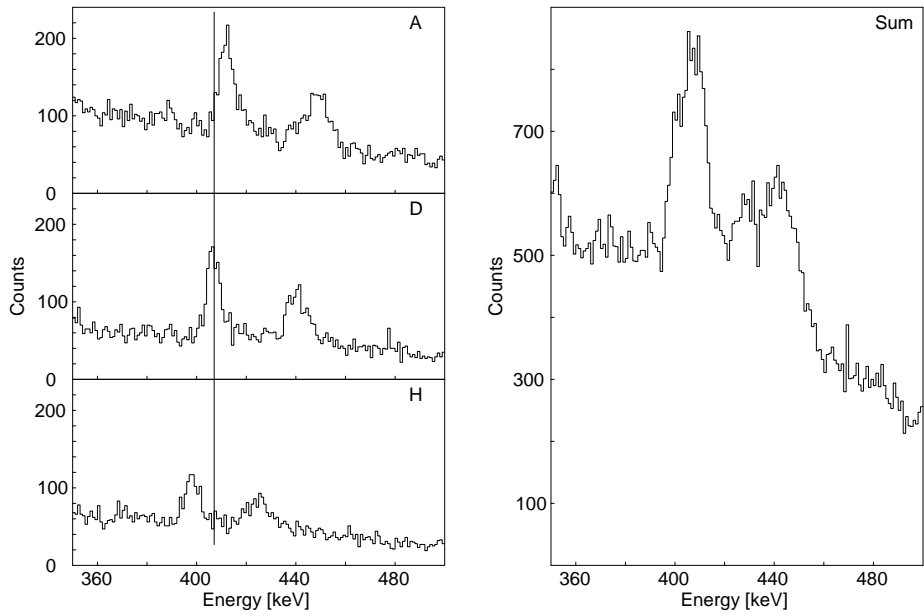


Fig. 5. Doppler shifted peaks observed at $d=10.5$ mm. The left panel shows spectra summed over φ for $\theta = 37^\circ$ corresponding to SeGA detector slices A, D, and H (for naming conventions of SeGA slices, see Ref. [8]). The right panel shows the sum of all spectra for the 37° SeGA ring.

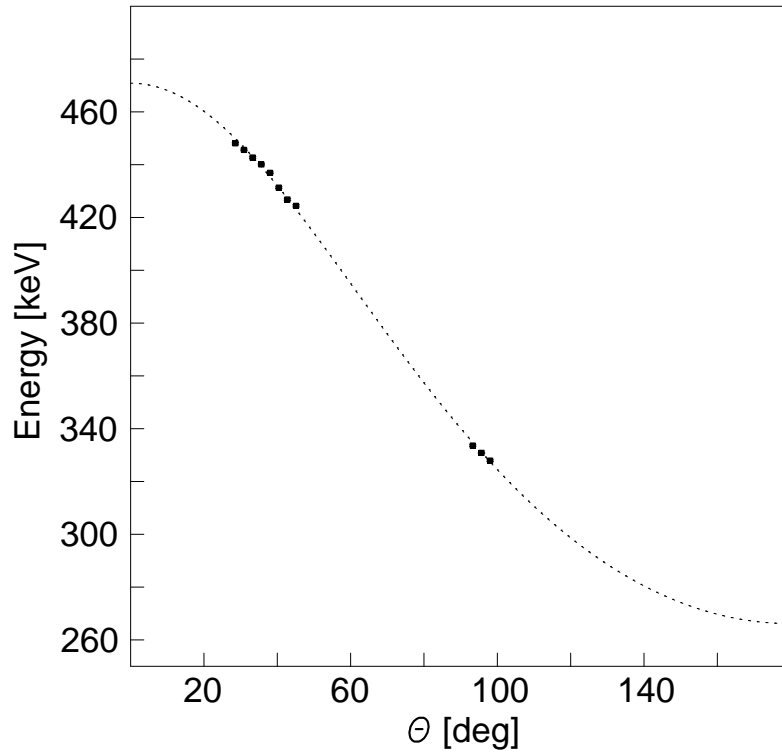


Fig. 6. The result of a least squares fit of gamma-ray energy vs. polar angle θ at $d=10.5$ mm for the peak corresponding to the decay between the target and the degrader. The data points are the γ -ray energies recorded by the SeGA array at different values of the polar angle θ . The dotted line is the least squares fit of Eq. 14 to these data points.

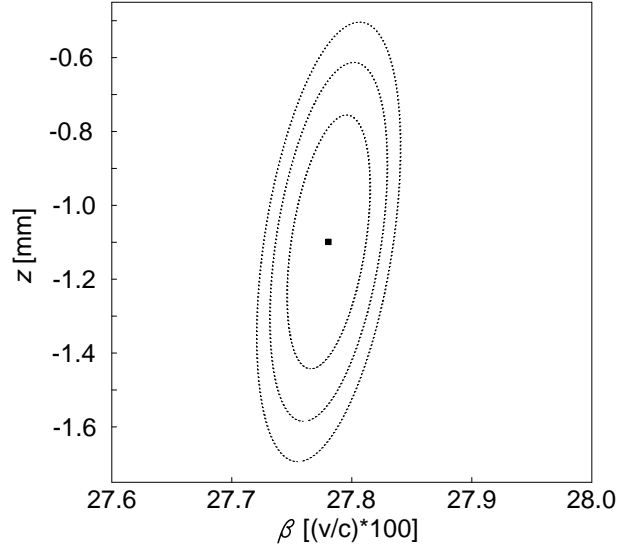


Fig. 7. The χ^2 contour plot of β_H vs. z_H resulting from the least squares fitting of γ -ray energy data for $d=10.5$ mm to Eq.14. The dotted ellipses around the calculated value of β_H and z_H correspond to 68.3%, 95.4%, and 99.7% confidence levels. Notice that the error on β_H is $< 0.5\%$ at 99.7% confidence level. This is strong evidence of the velocity measurement precision for the time of flight method.

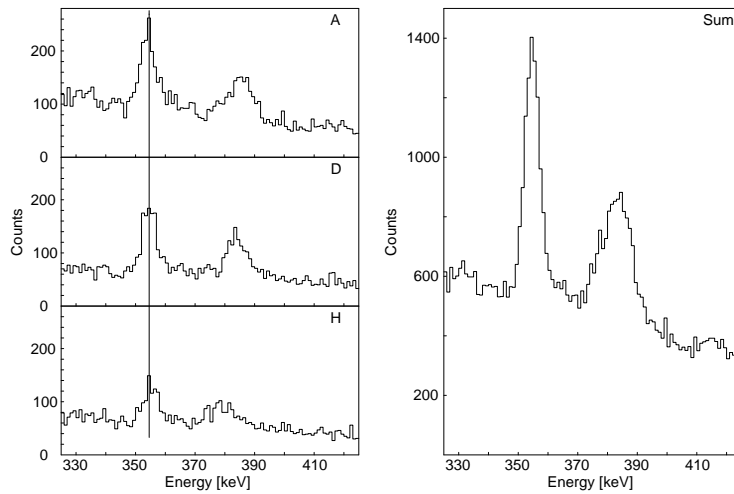


Fig. 8. Spectra corresponding to those shown in Fig. 5 but Doppler corrected using the β_L and z_L values measured for the decay downstream from the degrader. Notice the improvement in the signal to noise ratio for the low energy peak over Fig. 5.

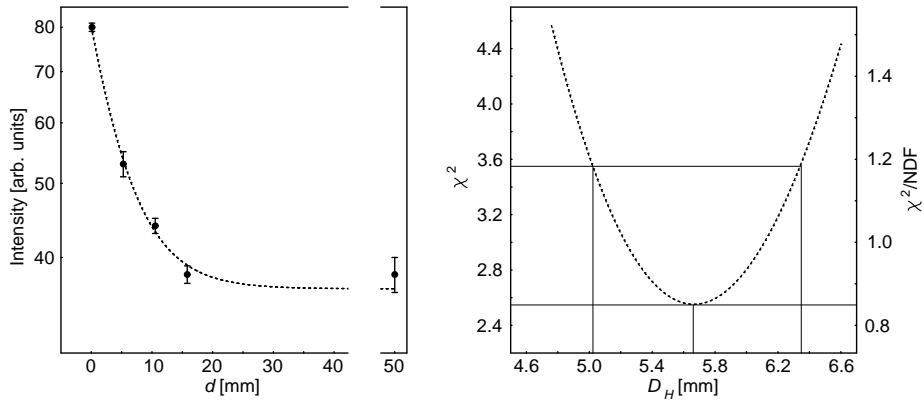


Fig. 9. Results of an exponent plus a constant fit of Eq. 16 to the N_H/N_0 data from Tab. 3. The extracted value of $D_H=5.6^{+0.8}_{-0.6}$ corresponds to the lifetime $\tau=64^{+10}_{-8}$ ps for $\beta_H=0.278(1)$.

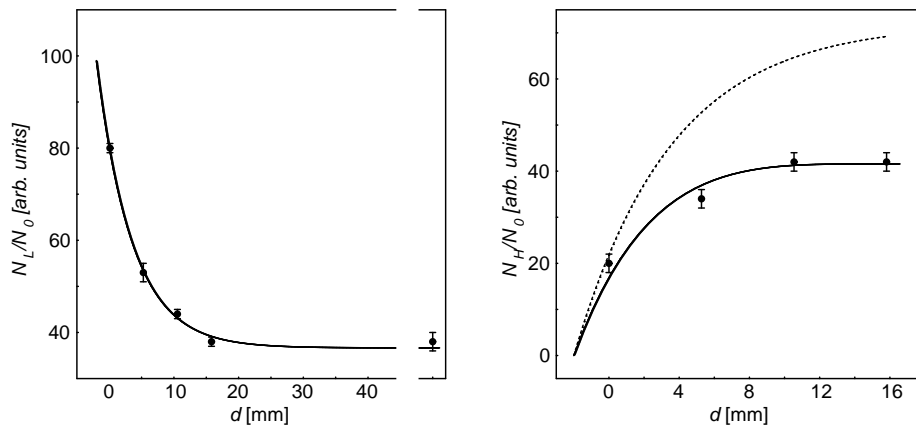


Fig. 10. Results of a simultaneous fit according to Eqs. 18 to the data from Tab. 3. The extracted value of $D_H=5.5(7)$ is consistent with that from the exponent plus a constant fit from Fig. 9 to the N_H/N_0 data only. The dashed line in the right panel corresponds to the curve expected in the absence of the efficiency loss for the decays between the target and the degrader.